DTU Library

Denaturation strategies for detection of double stranded PCR products on GMR magnetic biosensor array

Rizzi, Giovanni; Lee, Jung-Rok; Guldberg, Per; Dufva, Martin; Wang, Shan X.; Hansen, Mikkel Fougt

Link back to DTU Orbit

Denaturation strategies for detection of double stranded PCR products on GMR magnetic biosensor array

Giovanni Rizzi[1], Jung-Rok Lee[2], Per Guldberg[3], Martin Dufva[1], Shan X. Wang[2], Mikkel F. Hansen[1*]

[1]*Department of Micro- and Nanotechnology, DTU Nanotech, Technical University of Denmark, Building 345B, DK-2800 Kgs. Lyngby, Denmark*

[2]*Department of Materials Science and Engineering, Stanford University, Stanford CA, USA.*

[3]*Diet, Genes and Environment, Danish Cancer Society Research Center, Strandboulevarden 49, DK-2100 Copenhagen, Denmark*

*Corresponding author: Mikkel F. Hansen, +45 4525 6338
E-mail addresses: giori@nanotech.dtu.dk (G. Rizzi); jungrok@stanford.edu (J.-R. Lee); perg@cancer.dk (P. Guldberg); martin.dufva@nanotech.dtu.dk (M. Dufva); sxwang@stanford.edu (S.X. Wang); mikkel.hansen@nanotech.dtu.dk (M.F. Hansen)

Abstract
Microarrays and other surface-based nucleic acid detection schemes rely on the hybridization of the target to surface-bound detection probes. We present the first comparison of two strategies to detect DNA using a giant magnetoresistive (GMR) biosensor platform starting from an initially double-stranded DNA target. The target strand of interest is biotinylated and detected by the GMR sensor by linking streptavidin magnetic nanoparticles (MNPs) to the sensor surface. The sensor platform has a dynamic detection range from 40 pM to 40 nM with highly reproducible results and is used to monitor real-time binding signals. The first strategy, using off-chip heat denaturation followed by sequential on-chip incubation of the nucleic acids and MNPs, produces a signal that stabilizes quickly but the signal magnitude is reduced due to competitive rehybridization of the target in solution. The second strategy, using magnetic capture of the double-stranded product followed by denaturing, produces a higher signal but the signal increase is limited by diffusion of the MNPs. Our results show that both strategies give highly reproducible results but that the signal obtained using magnetic capture is higher and insensitive to rehybridization.

1 Introduction

Allele specific hybridization of DNA to surface-tethered complementary probes is the underlying principle of the DNA microarray assay, which is the standard tool for genetic studies. The strength of this technique lies in its capability of detecting low concentrations of target DNA with single nucleotide specificity. Microarrays are applied to, for example, the diagnosis of cancer and genetic diseases (Albertson and Pinkel, 2003; Ramaswamy *et al.*, 2002; Schena *et al.*, 1995; van 't Veer *et al.*, 2002). Microarray-like assays have been implemented in lab-on-a-chip devices aiming to decrease equipment cost, increase sensitivity, and reduce assay time to further enable diagnostic applications (Liu *et al.*, 2004; Trau *et al.*, 2002; Wang, 2000). Microfluidics has been employed to automate sample handling and to decrease assay time via mixing or driven sample flows to overcome diffusion limitations during hybridization (Wang and Li, 2011). Surface-based sensing methods rely on hybridization strategies that are optimal to detect single stranded DNA (ss-DNA), but often a double stranded DNA (ds-DNA) product is available from genomic DNA or PCR amplification. For ds-DNA, the standard procedure is to denature the sample at high temperature (90-95 °C) prior to hybridization. The sample is then shock-cooled to reduce diffusion and thereby re-hybridization in solution. Nevertheless, re-hybridization in solution will still compete against target hybridization to surface-bound probes. Since hybridization in solution is generally faster than to the surface, several other approaches have been employed to increase assay sensitivity. Servoli *et al.*(2012) repeatedly heat denatured the target ds-DNA and exposed the solution to the hybridization substrate after each heat treatment. Furthermore, asymmetric PCR can be employed to produce ss-DNA during PCR amplification (Wei *et al.*, 2004) or dsDNA can serve as template for an in vitro transcription reaction producing a large amount of single stranded RNA (Petersen *et al.*, 2008).

Here, we study and compare two techniques to denature ds-DNA PCR products into ss-DNA. In addition to the standard heat and shock cooling denaturation strategy, we test denaturation of magnetically labeled ds-DNA target, which is magnetically trapped in a separation column. This removes the unlabeled, reverse PCR strand that would otherwise compete with surface-bound probes. The advantages and disadvantages of the two approaches are compared for the detection of DNA target using a GMR biosensor array, which monitors the surface binding in real time.

2

2   Experimental

2.1   GMR magnetic biosensor setup

GMR magnetic biosensor array chips, each comprising 64 sensors (Osterfeld *et al.*, 2008), were used to detect the biotinylated DNA target conjugated with streptavidin-coated magnetic nanoparticles (MNPs). After activation of the sensor surface with NHS-EDC chemistry as described by Kim *et al.* (2013), the active area of each sensor was functionalized with amino-modified DNA probes by spotting about 1.5 nL of a 20 μM probe solution in 3×SSC buffer using a robotic spotter (Scienion, sciFlexarrayer). Subsequently, the sensor surface was washed in Phosphate buffered saline (PBS) with 0.1 % Bovine serum albumin (BSA) and 0.05 % Tween-20, and blocked with 1 % BSA. A sample well was installed on each sensor chip to facilitate exposure to liquid samples.

Hybridization of complementary biotinylated target from the sample to the probes on the sensor surface and labeling of this target with streptavidin MNPs produced a change in the magnetoresistance ratio of the GMR sensor (schematic in **Figure 1**). This was measured as follows: The sensors were biased with a voltage at a frequency of f_1=540 Hz or 590 Hz. An external Helmholtz coil supplied an alternating magnetic field of amplitude 3 mT at a frequency f_2 = 210 Hz. MNPs near the sensor surface magnetized by the external AC field generate a stray field acting on the GMR biosensors (Lee *et al.*, 2016). The MNP signal was measured in the sensor signal at f_1+f_2 (Osterfeld *et al.*, 2008). The signal at f_1 is proportional to the resistance of the GMR sensor and was used to measure the sensor temperature and to correct for the temperature dependence of the MR signal (Hall *et al.*, 2010). The MR ratio, *MR*, is defined as the ratio of the signals measured at f_1+f_2 and f_1. The MR ratio measured prior to injection of MNPs is denoted MR_0. The binding of MNPs to the sensor results in a change $\Delta MR = MR - MR_0$ of the *MR* ratio. The binding signal was taken as $\Delta MR/MR_0$ as this compensates for possible variations in MR_0, i.e., $\Delta MR/MR_0$ measures the strengthening of the external applied magnetic field due to the presence of MNPs. It has previously been shown that $\Delta MR/MR_0$ is proportional to the amount of beads bound to the sensor surface and also that this signal is only very weakly affected by a background from a dilute suspension of MNPs over the sensor (Wang and Li, 2008; Yu *et al.*, 2008).

The sensor temperature was controlled using the custom built chip-holder shown in **Figure 1a**. The temperature of the aluminum chip-holder, in good thermal contact to the chip was controlled by a Peltier element and a Pt control thermometer. An LFI3751 control unit (Wavelength Electronics, USA) was used to implement feedback control and monitor the chip temperature.

2.2 Detection of synthetic ss-DNA target

Sensors were functionalized as described above with probes 1-3 as well as a biotinylated DNA strand (positive reference) and a DNA strand not matching the target (negative reference). The target used was a 120 base long synthetic ss-DNA biotinylated at the 5' end to allow for magnetic labelling. All sequences are given in the Supplementary Information, **Table S1**. Seven concentrations of target DNA from $c = 0$ to $c = 40$ nM were measured. First, a volume of 50 µL 2×SSC with target was incubated on the sensor array for 1h at 37°C with gentle shaking. After hybridization, unbound sample was washed with 750 µL of 4×SSC leaving 50 µL of buffer in the sample well. Then, 50 µL of stock solution of streptavidin microbeads (Miltenyi Biotec, 130-048-101) with a diameter of 50 nm was added to the sensor and the signal was monitored at 37°C for 30 min. Further information on the magnetic particles is given in the Supplementary Information, Table S2. All experiments were carried out using streptavidin MNPs as magnetic labels.

2.3 Detection of ds-DNA from PCR products

For the detection of PCR products, four sensors were functionalized with each detection probe as well as with a biotinylated positive reference probe and a negative reference probe with a sequence non-complementary to those of the PCR products. Two probes designed to genotype of the *BRAF* c.1799 T>A single base substitution in the human *BRAF* gene were used (**Table S3**). The wild type (WT) and mutant type (MT) probes are complementary to the WT and MT target DNA sequences, respectively.

A 167 bp segment of Exon 15 of the human *BRAF* gene was amplified for cell line EST100 from the European Searchable Tumor Line Database (ESTDAB). Genomic DNA was extracted using Qiagen AllPrep DNA/RNA/Protein Mini kit (Qiagen GmbH, Hilden, Germany). PCR was performed using a Veriti™ 96-Well Thermal Cycler (Applied Biosystems) and TEMPase Hot Start Polymerase (VWR). The primer sequences are given in **Table S3**. Amplification was run for 40 cycles of 95°C for 30 s, 56°C for 30 s and 72°C for 30s. The ds-DNA PCR products were denatured using two different strategies, as schematically illustrated in **Figure 2**, to facilitate hybridization of the single sided PCR product to the detection probes on the GMR biosensor array. All measurements were carried out in a background of MNPs in suspension.

Denaturation strategy 1: Heat and shock cooling
Figure 2a shows the heat and shock cooling denaturation approach. Ethylenediaminetetraacetic acid (EDTA) was added to 50 µL of PCR products to a final EDTA concentration of 10 mM. EDTA was used to sequester Mg and inhibit polymerase. The sample was heated to 90°C for 3 min to denature ds-DNA. Subsequently, it was

shock-cooled to 5°C for 1 min to slow down re-hybridization. The sample ionic strength was then adjusted by addition of 10 µL of 20×SSC and the solution was pipetted into the sensor reaction well. The target hybridization took place in an incubator at 37°C for 1 h. The GMR array chip was washed with 750 µL of 4×SSC leaving a volume of 50 µL buffer. Finally, 50 µL stock solution of MNPs was added and these were allowed to bind to the biotinylated primer of the forward amplicon strand hybridized to the sensor surface. The $\Delta MR/MR_0$ signal was monitored in real time at 37°C for 30 min after the MNPs were added and the binding signal was taken as the value at $t = 30$ min.

Denaturation strategy 2: Magnetic column separation and denaturation

Figure 2b shows the process used for denaturation of ds-DNA amplicons using magnetic column separation. First, 50 µL of PCR products was magnetically labeled off-chip with 50 µL stock solution of MNPs at 37°C for 30 min. Subsequently, the DNA labeled with MNPs was magnetically trapped in a MACS µColumn (No. 130-042-701, Miltenyi Biotec). The ds-DNA was denatured by washing the column with 2 mL of 6 M urea in DI water at 75°C. Urea was here used to reduce the melting temperature of the double-stranded amplicons. Then, the forward PCR strands labeled with MNPs were eluted from the column with 100 µL of 2×SSC buffer. Finally, the sample was injected in the sensor well and the $\Delta MR/MR_0$ signal from hybridization of magnetic labeled ss-DNA was monitored in real time at 37°C for 1 h.

3   Results

3.1   Dose-response curve for detection of synthetic ss-DNA

To evaluate the sensitivity and dynamic range of the GMR sensor platform for DNA detection, we first characterized the allele specific hybridization of a synthetic biotinylated ss-DNA target to the various probes tethered to the surface of the GMR sensors. Three probes with different lengths and C+G contents as well as positive and negative reference probes (**Table S1**) were immobilized on the sensors with four replicates. The $\Delta MR/MR_0$ signal was monitored during magnetic labelling of hybridized targets (30 min). A four-fold serial dilution of targets from 40 nM to 39 pM and a zero analyte sample were measured.

Figure 3 shows the end-point (30 min) hybridization signals for the three different probes for a dilution series of ss-DNA. Error bars represent the standard deviation (SD) of four identical sensors (n=4). Due to the high affinity of streptavidin-biotin bond, the signal reached its steady-state value in less than 30 min after addition of MNPs. The positive reference signal level was found to be consistent for all tested target concentrations.

Titration curves for all probes were well fitted with a logistic curve (full lines in **Figure 3**, parameters are given in **Table S4**). The signals from probes 1 and 2 assumed similar values for all target concentrations. For $c \geq 1$ nM, the signal from probe 3 was found to be significantly higher than those from the other two probes. In particular, the signal from probe 3 approached the positive reference signal for $c = 40$ nM, indicating that the detection probes were close to being saturated with the target DNA. The signal from the zero analyte sample ($c = 0$, $n = 12$) was $\Delta MR/MR_0 \pm 1SD = (-0.016 \pm 0.009)$ %. The dashed line in **Figure 3** represents this signal plus two SDs defining the signal corresponding to the limit of detection (LOD). The lowest tested concentration $c = 39$ pM was found to give a significantly larger signal than that for $c = 0$ pM and thus the limit of detection (LOD) was below 39 pM.

3.2 Detection of ds-DNA PCR products

To measure DNA hybridization of PCR products to surface-tethered allele specific detection probes, we tested the two presented denaturation strategies.

Denaturation strategy 1: Heat and shock cooling

First, the ds-DNA hybrids were heat denatured at 90°C and re-hybridization was inhibited by shock cooling to 5°C. The sample was then hybridized on the sensor surface. The streptavidin MNPs were introduced after washing and their binding to the biotinylated amplicons hybridized to the surface was monitored in real time. **Figure 4a** shows $\Delta MR/MR_0$ vs. time t after the MNPs were introduced. The signal was measured for WT and MT probes targeting the *BRAF* c.1799 A>T mutation as well as for a biotinylated positive reference probe and a non-complementary negative reference probe. The negative probe signal maintained a value near zero throughout the experiment and was thus not affected by the suspension of MNPs over the sensor. The signal from the positive reference as well as from the WT and MT probes increased steeply after MNP injection (t=0) and stabilized in 5-10 min. The signals from the WT and MT probes reached nearly identical values after the hybridization under low stringency conditions.

Denaturation strategy 2: Magnetic column separation and denaturation

For the second denaturing strategy, the biotinylated forward strand of the PCR products was labeled with MNPs prior to introduction to the GMR sensor array. A magnetic separation column was used to trap the MNPs while the complementary strand was denatured with high stringency 75°C 6M urea. Following denaturation, the MNP-labeled ss-DNA was eluted from the column and injected on the GMR biosensor array. **Figure 4b** shows the magnetic signal measured during hybridization of labeled DNA for WT, MT, positive and negative reference probes. The signals from sensors with WT, MT and positive reference probes increased steadily throughout the experiment. No difference

was observed between the signals from the WT and MT probes and their values increased linearly with time up to at least $t = 60$ min. The signal from the positive reference was found to increase at a lower rate than in the previous heat denaturation experiment and also did not reach saturation after 60 min.

Comparison of denaturation strategies

Figure 5 shows the end-point values for the indicated detection probes for the two techniques. Error bars are one SD obtained from four nominally identical sensors on each chip. Using both strategies, all detection probes resulted in sensor responses that were highly reproducible. The signals from the sensors functionalized with WT and MT probes were indistinguishable after hybridization at low stringency and reached about 20% of that from the positive reference in the experiment. Using the magnetic separation protocol, the end-point signals from the sensors with MT probes and the positive reference were roughly 20% higher than the corresponding signals obtained using denaturation strategy 1.

4   Discussion

4.1   Dose-response curve for detection of synthetic ss-DNA

DNA detection on GMR biosensor array was tested with synthetic ss-DNA. We obtained an LOD ≤ 39 pM and a dynamic range of concentrations of more than 1000. Compared to previous work by Xu *et al.* (2008), the hybridization reaction was performed in this study only for one hour, showing the feasibility of fast hybridization assays on GMR sensors. The dose-response curves differed strongly for the three probes due to the differences in length, C+G content and probe sequence. Although the longest probe (probe 3) showed the highest signal at all investigated concentrations, all probes resulted in similar LODs. Only the signal from probe 3 approached the positive reference value. For this probe, it was therefore possible to achieve a surface density of bound target giving rise to an amount of bound MNPs similar to that for the positive reference.

4.2   Strategies for detection of ds-PCR products

Both investigated denaturation strategies were found viable for detection of PCR products on the GMR biosensor array. The signals from identical sensors ($n = 4$) were found to be highly reproducible. The choice of biotinylated DNA as positive reference probe allowed for a quickly settling and stable reference signal in denaturation strategy 1. For both strategies, the negative reference produced a signal indistinguishable from the measurement noise.

Figure 4 presented the magnetic signal increase vs. time for both denaturation strategies. The observed signal increases differed greatly because of the different binding mechanisms for the two denaturation strategies. In heat denaturation, the measurements were performed during magnetic labelling of the target already hybridized to the surface probes. Hence, the final signal depended on the surface density of captured target and due to the high biotin-streptavidin affinity, the reaction kinetics was only limited by diffusion of MNPs to the sensor surface. Therefore, the signals from the WT and MT probes increased steeply immediately after bead injection and quickly reached their final values. The labelling with MNPs took place after washing. Therefore there was no biotinylated DNA in solution competing for the streptavidin binding. On the other hand, during hybridization, the entire solution of PCR products was injected on the surface. Thus, the surface detection probes competed with the reverse PCR strand for hybridization of the forward strand target. This competition limited the final surface binding signal.

In denaturation strategy 2, the real time signal of **Figure 4b** was measured while the MNP-labeled DNA hybridized to the sensor surface. During hybridization the target DNA as well as biotinylated primers were bound to MNPs. Thus the reaction kinetics was limited by both the lower affinity of DNA hybrids as well as translational and rotational diffusion of MNPs with DNA available for binding to the sensor surface. Nevertheless, the sample matrix during hybridization was much simpler than for denaturation strategy 1, because the magnetic separation removed the reverse PCR strand as well as un-used primers and the PCR buffer. Without the competing species, the hybridization signal increased linearly with time during the 60 min of hybridization and would saturate at a higher signal if incubated for even longer time. A similar argument is valid for the positive reference signal. After magnetic separation, the MNPs were decorated with target DNA as well as with biotinylated primers. This limits the number of sites on the MNPs available to link to the biotinylated positive reference probe. Therefore, the binding kinetics for the positive reference was slower than for denaturation strategy 1. We speculate that the lower saturation signal from the positive reference in denaturation strategy 1 was due to blocking of the positive reference probes by unspecific binding of other species in the complex sample matrix during hybridization.

Employing low stringency during hybridization allowed for a faster incubation. For both denaturation strategies, the endpoint signals for WT and MT probes for the *BRAF* c.1799 mutation were undistinguishable. After low stringency hybridization it was not possible to genotype SNPs since both perfectly matched and single point mismatched hybrids were stable in those conditions. We have previously demonstrated that single base mismatches can be detected using a magnetoresistive sensor platform by challenging the

8

hybrids with a stringent washing (Rizzi *et al.*, 2014) and/or increasing temperature (Rizzi *et al.*, 2015) to characterize the melting profiles for the WT and MT probes.

4.3 Consequences for biosensing applications

Both denaturation strategies showed strengths and weaknesses related to the reaction kinetics, particle diffusion and complexity of the matrix. Denaturation strategy 1 (heat denaturation) is simple and produces a fast signal increase during incubation of MNPs on the sensor. However, the signal is reduced and may be sensitive to the timing of the sample handling due to the competitive target in solution. Furthermore, components of the sample matrix, such as polymerase, may interfere with the analysis. Denaturation strategy 2 is operationally more complex due to the magnetic column separation and the signal increase during incubation on the sensor is at present limited by the diffusion of MNPs in solution. However, it offers a higher signal and allows for real time hybridization measurements that can be used for kinetic studies. Since the target is labeled with MNPs, it is potentially possible to integrate magnetic sample handling (van Reenen *et al.*, 2014) and magnetic focusing of the target to the surface (Graham et al., 2005; Morozov and Morozova, 2006) to automate sample preparation and enhance MNP diffusion to the surface. Such approaches may substantially reduce the incubation and analysis time.

5 Conclusions

The dynamic range and limit of detection of the giant magnetoresistive platform for detection of a single-stranded DNA target was characterized. The dynamic range covered at least three orders of magnitude from below 40 pM to above 40 nM with a 1h incubation time and results were found to be highly reproducible.

The sensor platform was used to compare two strategies to the detection of a biotinylated target, which was initially found as a double-stranded PCR product. The two strategies aim to denature PCR product to obtain ss-DNA for surface hybridization.

Both strategies gave highly reproducible results and took about 1.5 hours of processing from the initial PCR product to the final result. Shock cooling has the advantage that it is well established for microarray readouts but the disadvantage that it is less robust and produces lower signals due to rehybridization of the target in solution. The magnetic column separation provides an efficient separation and purification of the single-stranded target. This results in a higher signal with no interference from other components of the sample. However, disadvantages of the method are the longer required incubation time and the added cost of the magnetic separation column. Both protocols have the potential

to be substantially shortened, e.g., by reducing incubation times via active mixing (Wei et al., 2005) or by magnetic capture of the nanoparticles on the sensor surface (Morozov and Morozova, 2006).

The presented denaturation strategies and results are relevant for all surface-based hybridization assays for the detection of DNA, which is initially double-stranded, where magnetic nanoparticles are involved. This particularly involves all magnetoresistive sensor platforms. Our future work aims to use the presented methods for genotyping of mutations in DNA.

Acknowledgements

References

Albertson, D.G., Pinkel, D., 2003. Genomic microarrays in human genetic disease and cancer. Hum Mol Genet 12 Spec No, R145–52. doi:10.1093/hmg/ddg261

Graham, D.L., Ferreira, H.A., Feliciano, N., Freitas, P.P., Clarke, L.A., Amaral, M.D., 2005. Magnetic field-assisted DNA hybridisation and simultaneous detection using micron-sized spin-valve sensors and magnetic nanoparticles. Sens. Actuators B, Chem. 107, 936–944. doi:10.1016/j.snb.2004.12.071

Hall, D. a., Gaster, R.S., Osterfeld, S.J., Murmann, B., Wang, S.X., 2010. GMR biosensor arrays: Correction techniques for reproducibility and enhanced sensitivity. Biosens. Bioelectron. 25, 2177–2181. doi:10.1016/j.bios.2010.01.039

Kim, D., Marchetti, F., Chen, Z., Zaric, S., Wilson, R.J., Hall, D.A., Gaster, R.S., Lee, J.-R., Wang, J., Osterfeld, S.J., Yu, H., White, R.M., Blakely, W.F., Peterson, L.E., Bhatnagar, S., Mannion, B., Tseng, S., Roth, K., Coleman, M., Snijders, A.M., Wyrobek, A.J., Wang, S.X., 2013. Nanosensor dosimetry of mouse blood proteins after exposure to ionizing radiation. Sci. Rep. 3, 1–8. doi:10.1038/srep02234

Lee, J.-R., Sato, N., Bechstein, D.J.B., Osterfeld, S.J., Wang, J., Gani, A.W., Hall, D.A., Wang, S.X., 2016. Experimental and theoretical investigation of the precise transduction mechanism in giant magnetoresistive biosensors. Sci. Rep. 6, 18692. doi:10.1038/srep18692

Liu, R.H., Yang, J., Lenigk, R., Bonanno, J., Grodzinski, P., 2004. Self-Contained, Fully Integrated Biochip for Sample Preparation, Polymerase Chain Reaction Amplification, and DNA Microarray Detection. Anal. Chem. 76, 1824–1831. doi:10.1021/ac0353029

Morozov, V.N., Morozova, T.Y., 2006. Active bead-linked immunoassay on protein microarrays. Anal. Chim. Acta 564, 40–52. doi:10.1016/j.aca.2005.09.068

Osterfeld, S.J., Yu, H., Gaster, R.S., Caramuta, S., Xu, L., Han, S.-J., Hall, D. a, Wilson, R.J., Sun, S., White, R.L., Davis, R.W., Pourmand, N., Wang, S.X., 2008. Multiplex protein assays based on real-time magnetic nanotag sensing. Proc. Natl. Acad. Sci. U. S. A. 105, 20637–40. doi:10.1073/pnas.0810822105

Petersen, J., Poulsen, L., Petronis, S., Birgens, H., Dufva, M., 2008. Use of a multi-thermal washer for DNA microarrays simplifies probe design and gives robust genotyping assays. Nucleic Acids Res. 36, e10. doi:10.1093/nar/gkm1081

Ramaswamy, S., Ross, K.N., Lander, E.S., Golub, T.R., 2002. A molecular signature of metastasis in primary solid tumors. Nat. Genet. 33, 49–54. doi:10.1038/ng1060

Rizzi, G., Østerberg, F.W., Dufva, M., Fougt Hansen, M., 2014. Magnetoresistive sensor for real-time single nucleotide polymorphism genotyping. Biosens. Bioelectron. 52, 445–51. doi:10.1016/j.bios.2013.09.026

Rizzi, G., Østerberg, F.W., Henriksen, A.D., Dufva, M., Hansen, M.F., 2015. On-chip magnetic bead-based DNA melting curve analysis using a magnetoresistive sensor. J. Magn. Magn. Mater. 380, 215–220. doi:10.1016/j.jmmm.2014.09.004

Schena, M., Shalon, D., Davis, R.W., Brown, P.O., 1995. Quantitative monitoring of gene expression patterns with a complementary DNA microarray. Science 270, 467–70. doi:10.1126/science.270.5235.467

Servoli, E., Feitsma, H., Kaptheijns, B., Zaag, P.J. van der, Wimberger-Friedl, R., 2012. Improving DNA capture on microarrays by integrated repeated denaturing. Lab Chip 12, 4992. doi:10.1039/c2lc40691h

Trau, D., Lee, T.M.H., Lao, A.I.K., Lenigk, R., Hsing, I.-M., Ip, N.Y., Carles, M.C., Sucher, N.J., 2002. Genotyping on a Complementary Metal Oxide Semiconductor Silicon Polymerase Chain Reaction Chip with Integrated DNA Microarray. Anal. Chem. 74, 3168–3173. doi:10.1021/ac020053u

van 't Veer, L.J., Dai, H., van de Vijver, M.J., He, Y.D., Hart, A.A.M., Mao, M., Peterse, H.L., van der Kooy, K., Marton, M.J., Witteveen, A.T., Schreiber, G.J., Kerkhoven, R.M., Roberts, C., Linsley, P.S., Bernards, R., Friend, S.H., 2002. Gene expression profiling predicts clinical outcome of breast cancer. Nature 415, 530–536. doi:10.1038/415530a

van Reenen, A., de Jong, A.M., den Toonder, J.M.J., Prins, M.W.J., 2014. Integrated lab-on-chip biosensing systems based on magnetic particle actuation--a comprehensive review. Lab Chip 14, 1966–86. doi:10.1039/c3lc51454d

Wang, J., 2000. From DNA biosensors to gene chips. Nucleic Acids Res. 28, 3011–3016. doi:10.1093/nar/28.16.3011

Wang, L., Li, P.C.H., 2011. Microfluidic DNA microarray analysis: A review. Anal. Chim. Acta 687, 12–27. doi:10.1016/j.aca.2010.11.056

Wang, S.X., Li, G., 2008. Advances in Giant Magnetoresistance Biosensors With Magnetic Nanoparticle Tags: Review and Outlook. IEEE Trans. Magn. 44, 1687–1702. doi:10.1109/TMAG.2008.920962

Wei, C.-W., Cheng, J.-Y., Huang, C.-T., Yen, M.-H., Young, T.-H., 2005. Using a microfluidic device for 1 l DNA microarray hybridization in 500 s. Nucleic Acids Res. 33, e78–e78. doi:10.1093/nar/gni078

Wei, Q., Liu, S., Huang, J., Mao, X., Chu, X., Wang, Y., Qiu, M., Mao, Y., Xie, Y., Li, Y., 2004. Comparison of Hybridization Behavior between Double and Single Strand of Targets and the Application of Asymmetric PCR Targets in cDNA Microarray. J.

Biochem. Mol. Biol. 37, 439–444. doi:10.5483/BMBRep.2004.37.4.439

Xu, L., Yu, H., Akhras, M.S., Han, S.-J., Osterfeld, S., White, R.L., Pourmand, N., Wang, S.X., 2008. Giant magnetoresistive biochip for DNA detection and HPV genotyping. Biosens. Bioelectron. 24, 99–103. doi:10.1016/j.bios.2008.03.030

Yu, H., Osterfeld, S.J., Xu, L., White, R.L., Pourmand, N., Wang, S.X., 2008. Giant magnetoresistive biosensors for molecular diagnosis: surface chemistry and assay development. Proc. SPIE 7035, 70350E–70350E–9. doi:10.1117/12.794434

Supplementary info:

Table S1 – sequences of all probes used for ss-DNA measurements
   sequences probes 1-3, pos reference, target

Table S2 – Information on Miltenyi Microbeads

Table S3 – Sequences of all probes used for ds-DNA measurements

Table S4 – parameters of fits to 4-parameter logistic function

Denaturation strategies for detection of double stranded PCR products on GMR magnetic biosensor array

Giovanni Rizzi[1], Jung-Rok Lee[2], Per Guldberg[3], Martin Dufva[1], Shan X. Wang[2], Mikkel F. Hansen[1]

[1]*Department of Micro- and Nanotechnology, DTU Nanotech, Technical University of Denmark, Building 345B, DK-2800 Kgs. Lyngby, Denmark*

[2]*Department of Materials Science and Engineering, Stanford University, Stanford CA, USA.*

[3]*Diet, Genes and Environment, Danish Cancer Society Research Center, Strandboulevarden 49, DK-2100 Copenhagen, Denmark*
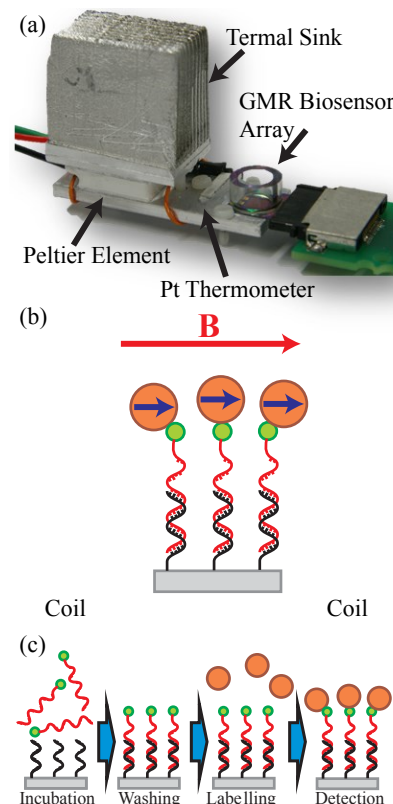
Figure 1: (a) GMR biosensor array chip mounted in temperature controlled chip holder. The chip-holder temperature is monitored via a Pt thermometer and regulated using a Peltier element. **(b)** Detection principle. Streptavidin-MNPs are linked to the GMR sensor surface via binding to a biotinylated DNA target hybridized to surface-tethered probes. The MNPs are detected by the magnetoresistive sensor as a perturbation of the magnetic field applied by external Helmholtz coils. **(c)** Schematic procedure for measurement of the hybridization of synthetic ss-DNA. The biotinylated target DNA is hybridized to the surface probes. After washing, streptavidin MNPs are introduced and the signal change is detected at the end-point of the incubation.
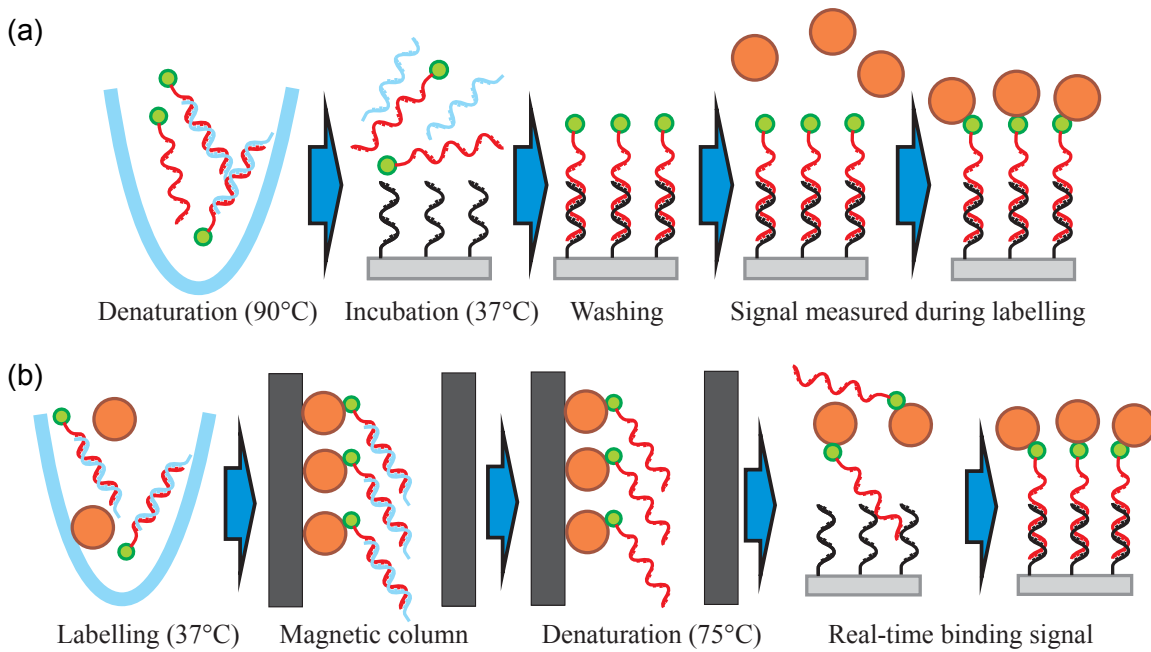
Figure 2: The two strategies employed to obtain ss-DNA from ds-DNA PCR products. **(a)** Detection strategy 1: The PCR products are heated to 90°C, shock cooled and incubated on the sensor for 1h. After low stringency washing to remove unbound sample, Streptavidin MNPs are added and the signal is measured during magnetic labeling of the biotinylated target already bound to the sensor surface. **(b)** Detection strategy 2: The PCR products are incubated with MNPs and captured in a magnetic separation column. After denaturation of ds-DNA with 6M urea at 75°C, the MNPs labeled with forward strand are eluted and hybridized on the sensor. Here, the signal is measured during 1h hybridization of magnetically labeled target.
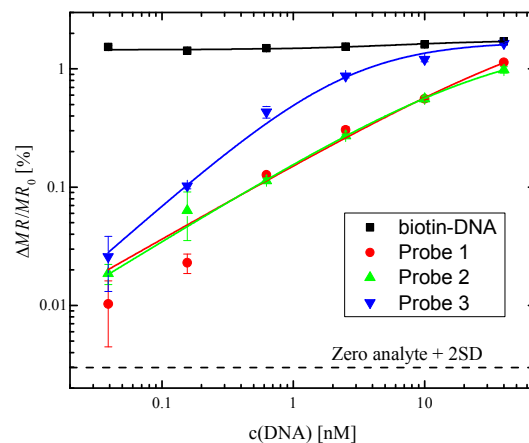

Figure 3: End-point detection of synthetic ss-DNA. GMR sensors were functionalized with probes 1-3 and biotinylated positive reference DNA. After 1h incubation of target DNA in a 4-fold dilution ladder from 40 nM to 39 pM, the signal was measured after washing unbound sample and adding MNPs over the sensor surface. Error bars are signal standard deviations (n = 4). The dashed line corresponds to the limit of detection, defined as the average zero-analyte signal for probes 1-3 plus two standard deviations (n=12). The curves are logistic function fits to the data (parameters in **Table S4**).
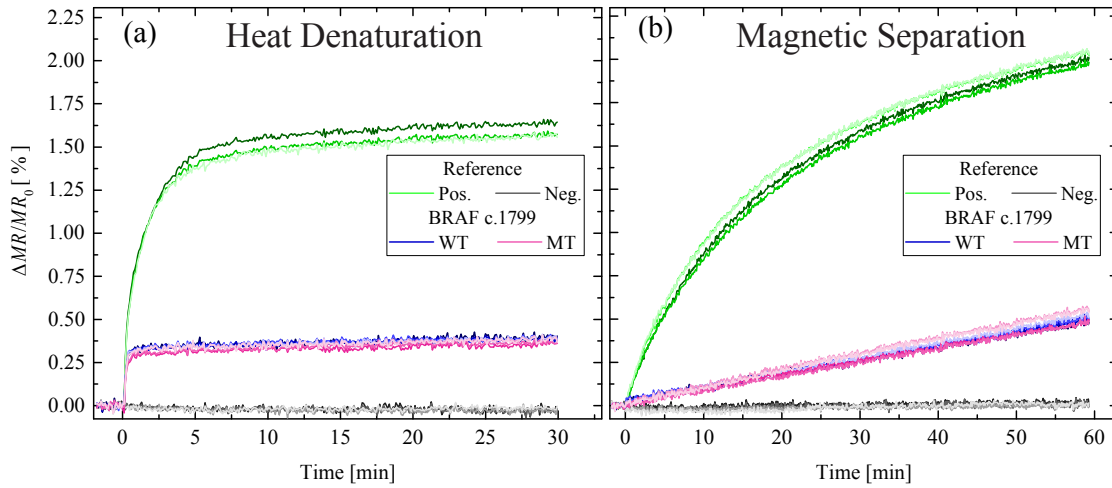
Figure 4: Real-time signals from GMR sensors for WT and MT probes for the *BRAF* c.1799 A>T mutation as well as positive and negative reference probes. (a) Results for denaturing strategy 1 (heat denaturation) where the signal is measured while labeling DNA hybridized to the sensor surface with MNPs. (b) Results for denaturing strategy 2 (magnetic separation) where the signal is measured during hybridization of MNP-conjugated DNA to the surface-tethered probes. All results are shown in triplicate with different brightness of the color for sensors with identical probes.
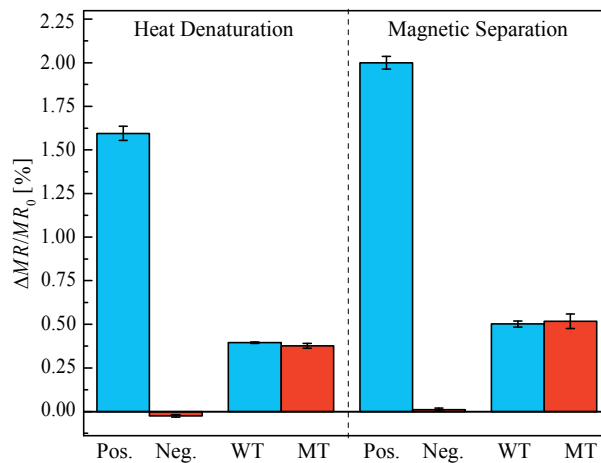

Figure 5: End-point signal after 30 min labeling (heat denaturation) or 60 min hybridization (Magnetic separation) over GMR biosensor array. Error bars are one standard deviation (*n* = 4). Signals were measured for WT and MT probes for the *BRAF* c.1799 A>T mutation as well as positive and negative reference probes.

Denaturation strategies for detection of double stranded PCR products on GMR magnetic biosensor array

Giovanni Rizzi[1], Jung-Rok Lee[2], Per Guldberg[3], Martin Dufva[1], Shan X. Wang[2], Mikkel F. Hansen[1]

[1]*Department of Micro- and Nanotechnology, DTU Nanotech, Technical University of Denmark, Building 345B, DK-2800 Kgs. Lyngby, Denmark*

[2]*Department of Materials Science and Engineering, Stanford University, Stanford CA, USA.*

[3]*Diet, Genes and Environment, Danish Cancer Society Research Center, Strandboulevarden 49, DK-2100 Copenhagen, Denmark*

Supplementary information

Table S1: DNA sequences of probes, reference and target for dose-response measurements on a single-stranded synthetic target.

Probe 1	NH2-C6-5'-(9×T) CCC TGT GGG GCA AGG TG -3'
Probe 2	NH2-C6-5'-(9×T) GAG GAG AAG TCT GCC GTT ACT G -3'
Probe 3	NH2-C6-5'-(9×T) GGC AGG TTG GTA TCA AGG TTA CA -3'
Biotin-DNA	NH2-C6-5'-(9×T)TGC GAG CTT CGT ATT ATG GCG -3'- TEG-biotin
Target	Biotin-5'-TCT CCT TAA ACC TGT CTT GTA ACC TTG ATA CCA ACC TGC CCA GGG CCT CAC CAC CAA CTT CAT CCA CGT TCA CCT TGC CCC ACA GGG CAG TAA CGG CAG ACT TCT CTT CAG GAG TCA GAT-3'

Table S2 – Information on Miltenyi Microbeads

The magnetic nanoparticles (MNPs) used for this work are MACS Streptavidin Microbeads (cat: 130-048-102, Miltenyi Biotec Norden AB, Lund, Sweden). The MNPs are composed of multiple iron oxide cores (Maghemite γ-Fe$_2$O$_3$) encapsulated in a polymer shell. The particle shell is functionalized with streptavidin for conjugation with biotinylated target. The numbers given in the table below were obtained from Bechstein *et al.* (2015), Koh and Sinclair (2007), and Koh (2008), where more information can be found. The binding capacity for biotinylated DNA was estimated to 90 molecules/MNP by measuring depletion of 20 nM biotinylated fluorescently labelled DNA (200 µL) upon addition of 0-5 µL stock solution of MACS Streptavidin Microbeads and subsequent magnetic column removal of MNP-DNA conjugates.

Nominal particle diameter	Measured particle diameter	Magnetic core diameter	Number of cores per particle	Particle number concentration (stock)	Particle magnetization	Saturation field
50 nm	46±13 nm	13±4 nm	11	$2\cdot10^{12}$ (mL)$^{-1}$	$2.47\cdot10^{4}$ A/m	$1.77\cdot10^{5}$ A/m

Table S2: Primers and probe sequences for *BRAF* c.1799 T>A amplification and genotyping.

Primers	fw	biotin- C6-5'- TTT TCC TTT ACT TAC TAC ACC TC -3'
BRAF Exon 15	bw	5'- GGA AAA ATA GCC TCA ATT CT -3'
Probes	WT	NH2-C6-5'-(9×T) TC CAT CGA GAT TTC ACT GTA GCT AGA C -3'
BRAF c.1799 T>A	MT	NH2-C6-5'-(9×T) CTC CAT CGA GAT TTC **T**CT GTA GCT AGA C -3'
References	Pos.	NH2-C6-5'-(9×T)TGC GAG CTT CGT ATT ATG GCG -3'- TEG-biotin
	Neg.	NH2-C6-5'-(9xT) GTG GGG CTA GGT G -3'

Table S3: Fitting parameters from logistic fit to dose response data for the three tested probes.
Equation: $y=A\ (x/x_0)^p/(1 + (x/x_0)^p)$

	A [‰]		x_0 [nM]		p	
	Value	Std. Error	Value	Std. Error	Value	Std. Error
Probe 1	37	28	147	266	0.632	0.083
Probe 2	18	2	32.7	7.2	0.683	0.017
Probe 3	17	1	2.54	0.56	0.981	0.070

References

Bechstein, DJ *et al.* 2015 High performance wash-free magnetic bioassays through microfluidically enhanced particle specificity. Sci Rep. 5, 11693. doi: 10.1038/srep11693.

Koh, A. L., Sinclair, R. 2007 TEM studies of iron oxide nanoparticles for cell labeling and magnetic separation. Technical Proceedings of the 2007 NSTI Nanotechnology Conference and Trade Show 4, 101-104.

Koh, AL 2008 Ph.D. Thesis, Electron microscopy investigations of nanoparticles for cancer diagnostic applications. ProQuest LLC, Ann Arbor MI.